Overtaking solitons of high energy in a one-dimensional Lennard-Jones chain

1980 J. Phys. A: Math. Gen. 13 1607

(http://iopscience.iop.org/0305-4470/13/5/020)

J. Phys. A: Math. Gen. 13 (1980) 1607–1621. Printed in Great Britain

Overtaking solitons of high energy in a one-dimensional Lennard–Jones chain

T P Valkering and C de Lange†

Department of Applied Physics, Twente University of Technology, PO Box 217, 7500 AE Enschede, The Netherlands

Received 18 June 1979

Abstract. The collision between two solitary waves in a one-dimensional Lennard–Jones chain of identical masses with nearest-neighbour interaction has been studied numerically. We consider two solitary waves of high energy travelling in the same direction such that they approach each other and collide. After collision there emerge again two solitary waves. A (small) disturbance, however, stays behind and the energy and momenta of the outcoming solitary waves are not equal to the corresponding quantities of the incoming ones. The effects are relatively small, however. Calculations are performed for different ratios of the velocity of the faster solitary wave to the velocity of the slower one. The effects mentioned above ultimately diminish if this ratio tends to unity. Further, we calculate the influence of shifting the initial position of one of the solitons for fixed initial position of the other one. The results are interpreted in terms of the individual motion of the particles.

1. Introduction

The occurrence of solitary waves, i.e. localised excitations that propagate without changing their shape, in a one-dimensional chain of identical masses with an anharmonic interaction potential is well known. Long low-wave models for such a chain, such as the Korteweg–de Vries (KdV) and the Boussinesq equations, have solitary wave solutions. The same holds for the exponential chain (Toda 1975). Solitary waves of high energy have been observed numerically in models with the Lennard–Jones and Morse potentials (Hardy and Karo 1977, Batteh and Powell 1978, Rolfe *et al* 1979). Further, it has been shown analytically (Valkering 1978) that periodic permanent waves occur in any chain with nearest-neighbour interactions of the Lennard–Jones type. If the energy per particle is high, the energy within one wavelength is strongly localised and the solution can be interpreted as a 'solitary' wave running through a closed circular chain.

In some of the cases mentioned above the solitary waves show the typical soliton behaviour, i.e. the equations admit solutions in which two different solitary waves approach each other, collide and emerge after collision with the same shapes and velocities as they had before. This type of behaviour has been found both analytically (in the KdV and Toda models) and numerically. In spite of these results, however, one may not expect that the exact soliton behaviour, as exhibited by the KdV and Toda models, holds true exactly for an arbitrary interaction potential.

† Present address: Institute of Theoretical Physics, University of Nijmegen, Toernooiveld, Nijmegen, The Netherlands.

In order to get some insight into this problem, we performed a set of calculations on two colliding solitary waves of high energy. We assumed nearest-neighbour interactions and a Lennard–Jones 6–12 potential. In particular, we considered the following three questions.

(i) If, after a collision, there exist again two solitary waves, what are their energies and momenta and is there transfer of momentum and energy to the underlying lattice?

(ii) Do the effects mentioned under (i) depend on the velocities of the incoming solitons, in particular on their ratio?

(iii) Do these effects depend on the distance between the solitary waves at the initial time†?

We calculated five series of collisions between two solitary waves with velocities C_F (the faster one) and C_S (the slower one) respectively. Each series is characterised by the quotient C_F/C_S which varies from 3·54 to 1·15, C_F having a fixed value. Within each series we varied the initial position of the faster wave, the initial position of the slower one being fixed. The results of the calculations are given in § 3.

For a good understanding of these results, we consider in § 2 the propagation of a single solitary wave of high energy. The energy in this case is concentrated mainly in one particle. The wave then propagates through the chain by repeated two-particle collisions in which the energy of the excited particle is transferred to the next particle, etc. The analysis in this section is based on Valkering (1978).

Finally, the results of § 3 will be interpreted starting from the picture of single solitary wave propagation described above. This will be done in § 4.

2. Solitary waves of high energy

In § 2.1 we shall give some analytic results, which are taken from Valkering (1978). Subsection 2.2 is devoted to the interpretation of these results in terms of the motion of a chain of hard spheres.

2.1. Analytical results

Consider a chain of unit masses with unit equilibrium distance between the particles. Let r_n denote the coordinate of the nth particle with respect to its equilibrium position and assume an interaction potential $V(r_n - r_{n-1})$. The equation of motion for the nth particle then reads

$$\ddot{r}_n = -V'(r_n - r_{n-1}) + V'(r_{n+1} - r_n). \tag{2.1}$$

The present calculations are performed with the Lennard–Jones potential (figure 1)

$$V(x) = \tfrac{1}{12}[(1+x)^{-12} - 2(1+x)^{-6} + 1]. \tag{2.2}$$

Consider a solution of (2.1) of the form

$$r_n(t) = r(\omega t - nk) + n\Delta \tag{2.3}$$

where r is a function of period 2π with zero average and where ω, k and Δ are real numbers. The form (2.3) represents a wave in the infinite chain with circular frequency and wavenumber ω and k respectively and average distance $1+\Delta$ between the particles.

† This effect cannot be excluded *a priori* because of the discreteness of the lattice.

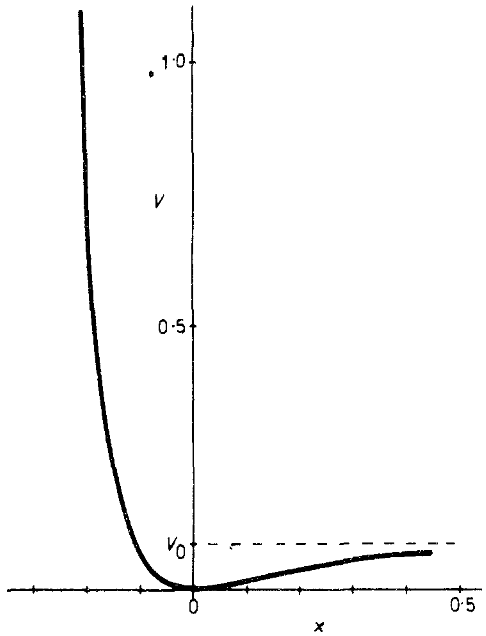

Figure 1. Lennard-Jones 6–12 potential. $V_0 = \frac{1}{12}$.

The parameter Δ gives the expansion of the chain per particle. Substitution of (2.3) in the equations of motion (2.1) yields, if $\omega t - nk$ is replaced by θ,

$$\omega^2(\mathrm{d}/\mathrm{d}\theta)^2 r(\theta) = -V'(r(\theta) - r(\theta+k) + \Delta) + V'(r(\theta-k) - r(\theta) + \Delta). \tag{2.4}$$

This equation is also found in the case of a closed circular chain of N particles at equilibrium distance $1+\Delta$, with deviation from the equilibrium position given by $r_n(t) = r(\omega t - nk)$, $k = 2\pi/N$, and with interaction potential

$$\tilde{V}(r_n - r_{n-1}) = V(r_n - r_{n-1} + \Delta) - V'(\Delta)(r_n - r_{n-1}). \tag{2.5}$$

The second term in the potential is added to guarantee that the potential has a minimum in the equilibrium position. The term cancels, however, in the equations of motion. We actually performed our calculations on such a closed chain.

From Valkering (1978, § 4) one easily obtains that (2.4) has a family of solutions

$$\{\omega^2(R), r(R, \theta)\}, \tag{2.6}$$

depending on a parameter, called R, satisfying

$$\frac{1}{2\pi}\int_{-\pi}^{+\pi} (\mathrm{d}r/\mathrm{d}\theta)^2\, \mathrm{d}\theta = R^2. \tag{2.7}$$

The range of R appears to be bounded:

$$0 \leq R < R_0 \qquad R_0 = (1+\Delta)N/(2\pi\sqrt{N-1}). \tag{2.8}$$

Note that this does not imply a physical restriction because the energy of the wave tends from zero to infinity in this range. The derivative $\mathrm{d}r/\mathrm{d}\theta$ is in $L_2[-\pi, +\pi]$ and one shows easily that r and $\mathrm{d}r/\mathrm{d}\theta$ are continuously differentiable.

Now we shall formulate some results for the case that R is close to R_0. These results are immediate consequences of Valkering (1978, theorems 6.1 and 6.2). The function $s_0(\theta)\in L_2[-\pi,+\pi]$ occurring in the following lines is defined by

$$s_0(\theta)=\frac{1}{2\pi}(1+\Delta)N \qquad |\theta|<\pi/N$$
$$=-\frac{1}{2\pi}(1+\Delta)\frac{N}{N-1} \qquad \text{elsewhere.} \tag{2.9}$$

Further, we assume that Δ, the average expansion of the chain per particle, does not exceed a certain value, say Δ_0, determined by $V''(\Delta_0)=0$ (cf Valkering 1978, theorem 4.4). For the present potential (2.2), it holds that $\Delta_0=(\frac{13}{7})^{1/6}-1=0{\cdot}1087$.

From the theorems mentioned above one derives easily the following proposition.

For any $\epsilon<0$ there is a solution $\{\omega^2(R'), r(R',\theta)\}$ such that

(i)

$$\left\|\frac{\mathrm{d}r}{\mathrm{d}\theta}-s_0\right\|\leqslant\epsilon R_0 \tag{2.10}$$

where $\|\ \|$ denotes the $L_2[-\pi,+\pi]$-norm,

(ii)

$$\sup_\theta\left|r(\theta+\tfrac{1}{2}k)-r(\theta-\tfrac{1}{2}k)-\int_{\theta-\frac{1}{2}k}^{\theta+\frac{1}{2}k}s_0(\tau)\,\mathrm{d}\tau\right|\leqslant\epsilon(1+\Delta), \tag{2.11}$$

(iii) and there exist positive numbers $M_{1,2}$ independent of ϵ such that

$$\omega^2>M_1+M_2\epsilon^{-m} \qquad m=12. \tag{2.12}$$

The inequality (2.12) expresses that ω^2 is unbounded in the limiting case considered here. Consequently the same holds for the energy of the wave (cf Valkering 1978, § 5). Further, note that m in (2.12) equals 12 because of the Lennard–Jones 6–12 potential and that (2.10) implies, together with (2.8),

$$0<R_0-R'\leqslant\epsilon R_0. \tag{2.13}$$

2.2. *The hard-sphere interpretation*

To give an interpretation of the results of § 2.1 we should realise that the velocity of the nth particle is approximately (in the sense of (2.10)) given by (cf (2.3))

$$\dot r_n(t)=\omega s_0(\omega t-nk) \qquad k=2\pi/N. \tag{2.14}$$

In an analogous way we have approximately (in the sense of (2.11))

$$r_n(t)-r_{n-1}(t)=\Delta+w_0(\omega t-nk+\tfrac{1}{2}) \tag{2.15}$$

in which $w_0(\theta)$ is given by

$$w_0(\theta)=-\int_{\theta-\frac{1}{2}k}^{\theta+\frac{1}{2}k}s_0(\theta')\,\mathrm{d}\theta'. \tag{2.16}$$

The functions $s_0(\theta)$ and $w_0(\theta)$ are shown in figure 2.

The right-hand sides of (2.14) and (2.15) describe a particular motion of a system of hard spheres with radius zero. This is represented schematically in figures 3 and 4.

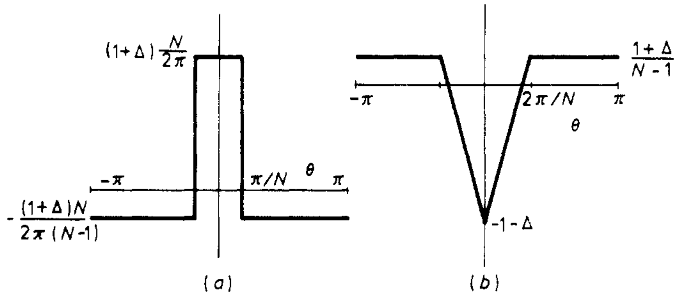

Figure 2. The functions $s_0(\theta)$ (a) and $w_0(\theta)$ (b) for $N=6$.

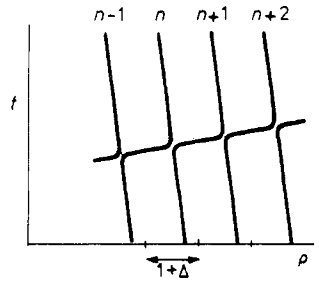

Figure 3. Coordinate–time diagram representing the propagation of a high-energy solitary wave in the chain. The coordinate ρ_n of the nth particle is given by $\rho_n \doteq n(1+\Delta)+r(\omega t-2\pi n/N)$.

Figure 4. Schematic representation of the propagation of a high-energy solitary wave. The arrows denote the velocities of the corresponding particles.

Figure 3 shows the coordinate–time diagram corresponding to the right-hand sides of (2.14) and (2.15). Figure 4 shows schematically the motion of a part of the chain.

Note that the propagation of the solitary wave through the chain is described essentially by repeated two-particle collisions in this high-energetic case. The $(n+1)$th particle (cf figure 4) moves with a velocity $\omega(1+\Delta)N/2\pi$ to the right (cf (2.14)). The other particles move with velocities $\omega(1+\Delta)N/2\pi(N-1)$ to the left. The distance $d_{i,i+1}$ between two neighbouring particles is given by (cf (2.15) and figure 2)

$$d_{i,i+1}=(1+\Delta)\frac{N}{N-1} \qquad i\neq n, n+1. \tag{2.17}$$

The fact that for $(R_0-R)/R_0 \ll 1$ the wave in the original chain can be approximated by a wave in a chain of hard spheres can be understood in the following way. If (2.3) is a solution of the original equations of motion, then

$$\bar{r}_n(t)=r(t-nk)+n\Delta \tag{2.18}$$

is a solution of a chain with interaction potential

$$\bar{V}(\bar{r}_n-\bar{r}_{n-1})=\omega^{-2}V(r_n-r_{n-1}). \tag{2.19}$$

If R tends to R_0 then ω^2 tends to infinity (cf (2.12)), so that $\bar{V}$ tends to a potential of hard spheres.

To conclude this section we consider the velocity of the wave. Obviously the phase velocity of the wave described in (2.3) is given by

$$C = \omega/k = N\omega/2\pi, \tag{2.20}$$

the dimension of which is 'number of particles per unit time'. One can also say that C gives the velocity in material coordinates. Correspondingly, the velocity in local coordinates, i.e. with respect to the external fixed frame of reference, equals $C(1+\Delta)$.

3. Collision of two solitary waves

3.1. *Qualitative description*

We start the calculation with two solitary waves that are separated completely in the practical sense and that propagate in the same direction such that the faster one overtakes the slower one. As time proceeds they collide and after collision there again appear two solitary waves. The calculations are stopped for times such that the outcoming solitary waves are separated again. A small disturbance is left behind, however, and the outcoming solitary waves are not the same as the incoming ones (cf figure 5). This behaviour differs from the behaviour exhibited by the KdV and Toda models, in which after collision the same solitons appear and in which there is no disturbance left behind. The differences, however, are relatively small as we shall see, which justifies the use of the term 'solitons' in the Lennard–Jones case as well.

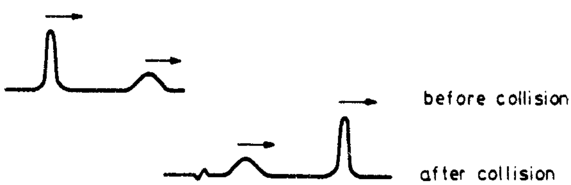

Figure 5. Schematic representation of a collision of two solitons.

It is not at all obvious that it is possible to speak of separated solitons in a finite chain. This possibility, however, is due to the fact that we are dealing with solitons of very high energy. Consider a single soliton. Its energy is almost completely concentrated within a small number, say four, of neighbouring particles. This is, in fact, a consequence of (2.10) and (2.11). Outside the excitation region the distance between two neighbouring particles equals a constant, say $\bar{d}$, which is given approximately by (2.17), whereas the velocities of the particles are equal. Because an additional constant velocity can be given to the whole chain without influence on the wave motion, the velocities of the particles outside the excitation can be chosen to be zero. From this point of view a soliton is an excitation propagating in a chain at rest with distance $\bar{d}$ between the particles. Then, however, it is also possible to consider two separated solitons propagating in the chain. Further, note that the velocity of a single soliton with respect to the fixed frame of reference equals $C\bar{d}$, where C is given by (2.20).

We performed five series of calculations, each series being characterised by the quotient C_F/C_S as described in the introduction. Within each series the initial position of the faster solitary wave varies over a distance, say d. The numerical results, however, are necessarily periodic in d, as the following argument shows. This period, say d_0, is given by

$$d_0 = \bar{d}\frac{C_F - C_S}{C_S}. \tag{3.1}$$

The essentials of the argument are that the fictitious position of the collision shifts with respect to the lattice if the initial distance varies, and further that two collisions are equivalent if the positions at which they take place are equivalent with respect to the lattice at rest, i.e. if their difference equals an integer times the particle distance $\bar{d}$ in the region at rest.

Let X_F and X_S denote the positions of the solitons at time $t=0$ with respect to the lattice. The solitons then collide at time t_0 (say),

$$t_0 = \frac{X_S - X_F}{C_F - C_S}\bar{d}^{-1}. \tag{3.2}$$

Consequently the collision takes place at position $X_C = X_S + t_0 C_S \bar{d}$. It follows that

$$X_C = X_S + C_S\frac{X_S - X_F}{C_F - C_S}. \tag{3.3}$$

If the position at time $t=0$ of the faster soliton is given by X'_F, we calculate X'_C in the same way and we get for the difference $X_C - X'_C$ (cf figure 6)

$$X_C - X'_C = C_S\frac{X'_F - X_F}{C_F - C_S}. \tag{3.4}$$

To be equivalent, $X_C - X'_C$ must be equal to an integer times $\bar{d}$, from which requirement (3.1) follows.

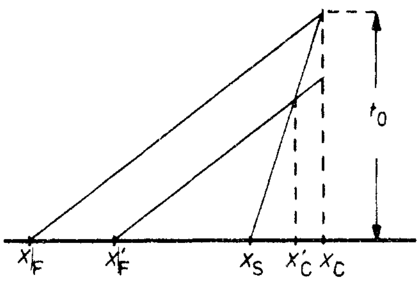

Figure 6. Fictitious position of the collision of solitons for different initial positions of the faster one.

3.2. *Quantitative description*

In order to describe the effects of the collisions quantitatively we define the momentum of a soliton as

$$M = \sum_{n_1}^{n_2} \dot{r}_n \tag{3.5}$$

where n_1 and n_2 are chosen in such a way that the excitation lies completely between the

n_1th and n_2th particles, i.e. these two particles are at rest within the calculational accuracy. In particular, we are interested in the quantities

$$\Delta M_{S,F} = M_{S,Fa} - M_{S,Fb} \qquad \Delta M_T = \Delta M_S + \Delta M_F, \tag{3.6}$$

where the subscripts a and b respectively denote 'after' and 'before' collision. For the high-energy solitons considered here, a value $n_2 - n_1 = 3$ appeared to be appropriate. Because of the centre-of-mass motion of the chain, M in (3.5) does not have a unique value. The differences in (3.6), however, are well defined.

In an analogous way we define the energy of the soliton as

$$E = \sum_{n_1}^{n_2} \tfrac{1}{2}\dot{r}_n^2 + \tfrac{1}{2}(\tilde{V}(r_{n+1} - r_n) + \tilde{V}(r_n - r_{n-1}) - 2\tilde{V}(0)) \tag{3.7}$$

where the potential $\tilde{V}$ (cf (2.5)) has been used to eliminate the energy corresponding to the average expansion $1 + \Delta$ of the chain. The quantities ΔE_T, etc, are then defined analogously to (3.6).

In the present case we have, the particles outside the excitation being at rest,

$$M_{Fb} = 1{\cdot}0 \times 10^2 \qquad E_{Fb} = 5{\cdot}0 \times 10^5 \qquad C_F = 12 \times 10^2. \tag{3.8}$$

Figure 7 shows ΔM_F and $-\Delta M_T$ as a function of d/d_0 for different values of C_F/C_S. Note that the vertical scales are the same in each case. One finds $-\Delta M_S$ by adding the corresponding graphs. More detailed numerical information about these calculations is given in table 1.

The graphs of ΔE_F and ΔE_S as a function of d/d_0 show qualitatively the same behaviour as those of ΔM_F and ΔM_S respectively. This is obvious because for any soliton E is a unique function of M so that for the small variations of M we are dealing with there exist some constants $\alpha_{F,S}$ such that

$$\Delta E_{F,S} \approx \alpha_{F,S} \Delta M_{F,S}. \tag{3.9}$$

The relation between ΔE_T and ΔM_T is not so simple of course. Figure 8 shows ΔE_T as a function of d/d_0 in the different cases. Table 2 gives some numerical values characterising the curves for ΔE.

To conclude this section we note on the one hand that the maximal values of the energy transfer to the lattice are large compared with V_0 (cf figure 1), such that the excitation which remains after the collision is a strongly nonlinear phenomenon. It is not a soliton, however (see the following section). On the other hand the energy transfer to the lattice is very small with respect to the energies of the interacting solitons. The same holds for the transfer of momentum. In fact this justifies the use of the term 'solitons' for the solitary waves considered here.

In the following section we consider the results in more detail.

4. Interpretation

If we consider figure 7, we observe that the shapes of the curves change for diminishing values of C_F/C_S. This can be explained after closer inspection of the collision process. This inspection also gives more insight into the fact that all values in tables 1 and 2 finally diminish for decreasing C_F/C_S. We start from the hard-sphere model described in § 2.

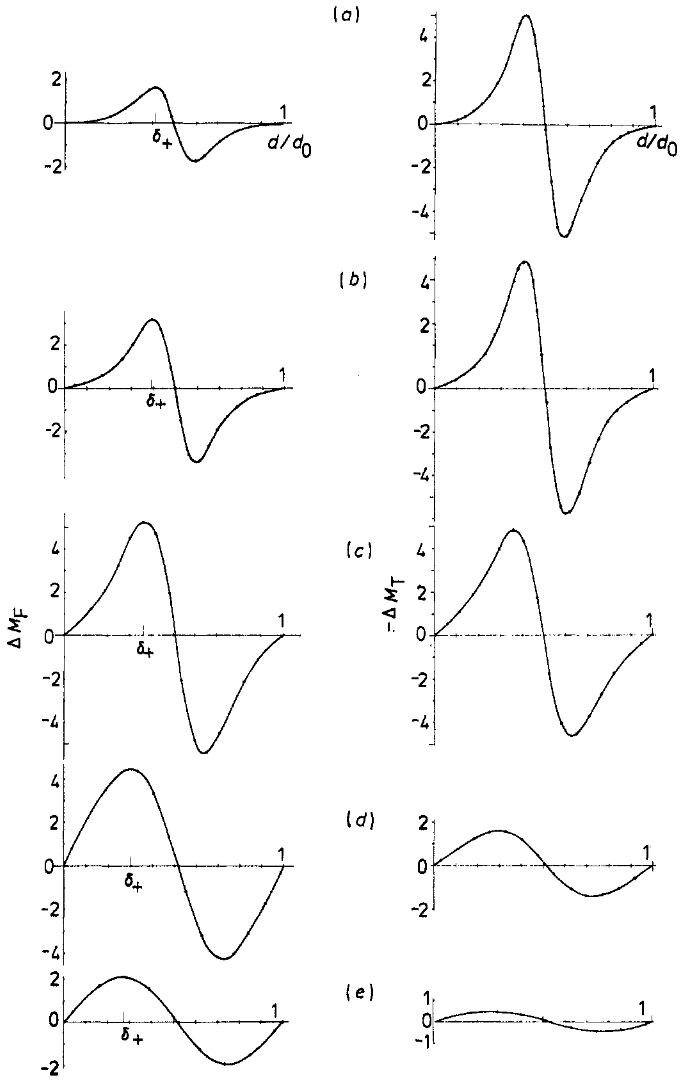

Figure 7. ΔM_F (left) and $-\Delta M_T$ (right) against d/d_0 for different values of C_F/C_S; (*a*)–(*e*) correspond to $C_F/C_S = 3{\cdot}45$, $2{\cdot}54$, $1{\cdot}73$, $1{\cdot}27$ and $1{\cdot}15$ respectively. For some precise values see table 1. Note that the dots correspond to the calculated values. The line connecting them is drawn to guide the eye.

The collision of two 'solitons' in a hard-sphere chain is represented schematically in figure 9. The two 'solitons' collide at a'. If a' does not coincide with one of the a_n, then the collision of the solitons is a simple two-particle collision in which the faster 'soliton' transfers its momentum and energy completely to the slower one and *vice versa*. If a' coincides with one of the a_i then the collision of the 'solitons' is a three-particle collision. Exchange of momentum and energy is governed by the corresponding conservation laws. The result is not unique. Certain bounds, i.e. values for $\Delta M_{F,S\pm}$, however, can be given (table 3). The behaviour of ΔM_F as a function of d/d_0 is given schematically in figure 10. Obviously, however, this figure is not realistic and for a

Table 1. Several quantities related to the ΔM curves. The different symbols are defined as follows. ΔM_{F+} is the maximum of ΔM_F, ΔM_{F-} is the minimum of ΔM_F, ΔM_{FR} is the maximum of $|\Delta M_F|/M_{Fb}$, ΔM_{TR} is the maximum of $|\Delta M_T|/(M_{Fb}+M_{Sb})$ and δ_+ is the value of d/d_0 for which ΔM_F attains its maximum. The other symbols are defined analogously.

C_F/C_S	δ_+	ΔM_{F+}	ΔM_{F-}	ΔM_{S+}	ΔM_{S-}	ΔM_{T+}	ΔM_{T-}	$\Delta M_{FR}\times 10^3$	$\Delta M_{SR}\times 10^3$	$\Delta M_{TR}\times 10^3$	M_{Sb}
3·46	0·41	1·6	−1·8	6·9	−6·6	5·2	−5·1	1·8	28	4·2	250
2·54	0·39	3·2	−3·4	9·3	−9·0	5·8	−5·9	3·4	26	4·3	360
1·73	0·36	5·3	−5·4	10·0	−10·0	4·6	−4·8	5·4	19	3·1	534
1·27	0·30	4·4	−4·3	5·7	−6·0	1·4	−1·6	4·4	7·9	0·9	745
1·15	0·27	2·1	−2·0	2·4	−2·6	0·4	−0·5	2·1	3·2	0·3	822

Table 2. Several quantities related to the ΔE curves. The symbol ΔE_{Tm} denotes the maximum of $|\Delta E_T|$. The other symbols are defined analogously to those in table 1.

C_F/C_S	$\Delta E_{F+}\times 10^{-3}$	$\Delta E_{F-}\times 10^{-3}$	$\Delta E_{S+}\times 10^{-3}$	$\Delta E_{S-}\times 10^{-3}$	ΔE_{Tm}	$\Delta E_{FR}\times 10^3$	$\Delta E_{SR}\times 10^3$	$\Delta E_{FR}\times 10^6$	$E_{Sb}\times 10^{-4}$
3·46	1·6	−1·8	1·8	−1·6	13·5	3·6	58	24	3·1
2·54	3·2	−3·4	3·4	−3·2	17·0	6·8	52	30	6·5
1·73	5·3	−5·4	5·4	−5·3	11·5	11	39	18	14
1·27	4·4	−4·2	4·2	−4·4	1·9	8·8	16	2·4	28
1·15	2·1	−2·0	2·0	−2·1	0·4	4·2	6·2	0·5	34

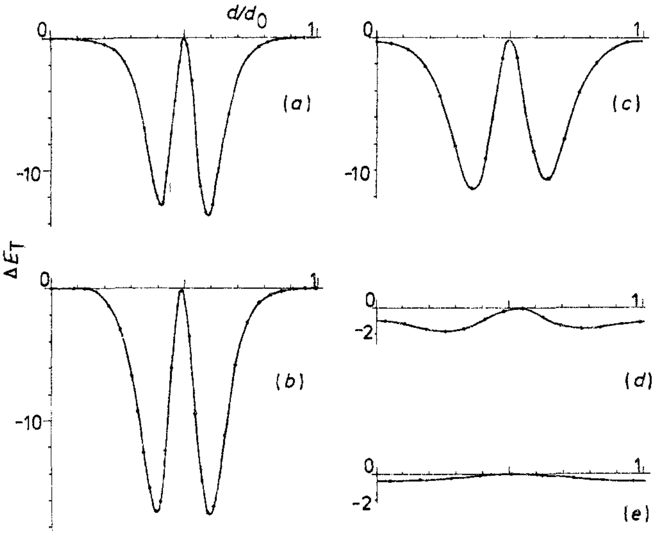

Figure 8. ΔE_T against d/d_0 for different values of C_F/C_S. The meaning of (a)–(e) is given in the caption to figure 7.

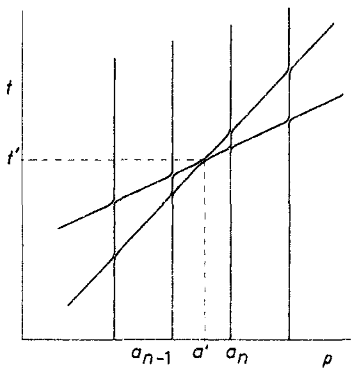

Figure 9. Coordinate–time diagram representing the collision of two 'solitons' in a hard-sphere chain (cf also figure 3).

near-hard-sphere chain, i.e. when the interaction forces have effectively a very small but non-zero range, one expects a figure like figure 11. Although one can no longer speak exactly of two- and three-particle collisions respectively, one can say that the flat part corresponds to a two-particle collision and the oscillatory part to a three-particle collision. One expects that this near-hard-sphere model applies in the case of solitons of high energy (cf § 2).

Now compare our numerical results, in particular figure 7, with figure 11. Indeed, we see that the case corresponding to the largest value of C_F/C_S is similar to figure 11. The resemblance disappears, however, for diminishing values of C_F/C_S. This is easily explained in the following way. For large C_F/C_S, the interaction time for two colliding particles (say for a collision at a', figure 9) is so short that the particles finish their

Table 3. Values of the bounds ΔM_{F+} etc for a hard-sphere chain. These values are calculated for $M_{Fb} = 1000$ and $M_{Sb} = M_{Fb}C_S/C_F$.

C_F/C_S	ΔM_{F+}	ΔM_{F-}	ΔM_{S+}	ΔM_{S-}	ΔM_{T+}	ΔM_{T-}
3·46	24	−273	379	−135	111	−106
2·54	46	−245	331	−183	137	−86
1·73	100	−184	220	−316	216	−36
1·27	204	−100	106	−469	265	−6
1·15	251	−63	64	−529	278	−1

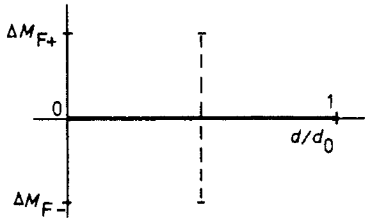

Figure 10. ΔM_F against d/d_0 for collisions of 'solitons' in a hard-sphere chain. The broken vertical line denotes the region of non-uniqueness.

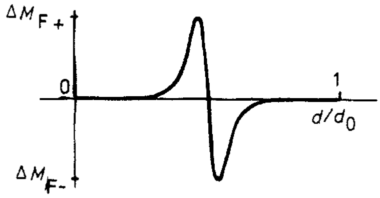

Figure 11. ΔM_F against d/d_0 for collisions of 'solitons' in a near-hard-sphere chain.

interaction before they meet the next particle at rest. If C_F/C_S diminishes, however, the time needed for a completed interaction grows, and finally the possibility of a two-particle interaction disappears and there are always three or more particles involved in the interaction between the solitons. The shapes of the curves $\Delta M_{F,S}$ then become more symmetric, i.e. the tops shift to $d/d_0 = 0{\cdot}25$ and $0{\cdot}75$ (table 1, second column).

This change of character of the collision process for diminishing C_F/C_S is found back in the velocity–time matrices given in tables 4 and 5.

First consider the case with the largest value of C_F/C_S (table 4). We see that the collision of the solitons is essentially a three-particle interaction. After the interaction one particle has a relatively low velocity and accounts for the disturbance of the lattice. If we look at table 5, however, we see that the collision between the solitons takes up a few particle distances and, correspondingly, that more particles are involved in the disturbance.

We conclude that the interpretation in terms of the individual motion of (near-)hard spheres gives a reasonable qualitative explanation of the results, at least for the larger values of C_F/C_S. A few remarks, however, must be made.

Table 4. Relative values of the velocities $\dot{r}_n(t)$ (upper part) and $r_{n+1}(t)-r_n(t)$ (lower part) as a function of time for a collision characterised by $C_F/C_S = 3{\cdot}46$ and $d/d_0 = 0{\cdot}38$. Time increases with a step equal to 10^{-3}. The actual values are the given ones multiplied by 10^{-1} and 10^{-3} respectively.

t \ n	1	2	3	4	5	6	7	8	9	10	11	12
1	9985	0	0	0	0	2498	0	0	0	0	0	0
2	0	9985	0	0	0	2357	142	0	0	0	0	0
3	0	0	9975	10	0	21	2478	0	0	0	0	0
4	0	0	0	8791	1194	0	2498	0	0	0	0	0
5	0	0	0	0	183	9802	2436	63	0	0	0	0
6	0	0	0	0	0	117	2798	9569	0	0	0	0
7	0	0	0	0	0	47	2436	0	10 000	0	0	0
8	0	0	0	0	0	47	2421	15	0	10 000	0	0
9	0	0	0	0	0	47	232	2204	0	0	9980	20
10	0	0	0	0	0	47	1	2436	0	0	0	7139
11	0	0	0	0	0	47	0	2432	5	0	0	0
12	0	0	0	0	0	47	0	773	1664	0	0	0

t \ n	1	2	3	4	5	6	7	8	9	10	11	12
1	−255	81	81	81	−258	−360	81	81	81	81	81	81
2	−275	−409	81	81	−10	−606	79	81	81	81	81	81
3	81	−121	−562	81	81	−537	−80	81	81	81	81	81
4	81	81	29	−709	78	−288	−330	81	81	81	81	81
5	81	81	81	81	−659	−143	−578	80	81	81	81	81
6	81	81	81	81	81	−582	−675	−125	81	81	81	81
7	81	81	81	81	87	−343	−280	−406	−278	81	81	81
8	81	81	81	81	92	−104	−524	81	−251	−433	81	81
9	81	81	81	81	96	61	−620	7	81	−96	−588	81
10	81	81	81	81	101	60	−383	−233	81	81	50	−725
11	81	81	81	81	106	56	−139	−477	81	81	81	81
12	81	81	81	81	110	51	69	−649	46	81	81	81
13	81	81	81	81	115	46	81	−430	−186	81	81	81
14	81	81	81	81	120	42	81	−186	−430	81	81	81
15	81	81	81	81	125	37	81	45	−649	69	81	81
16	81	81	81	81	129	32	81	81	−477	−139	81	81

First note the oscillatory character of the disturbance of the chain after collision (cf table 6). This accounts at least partially for the diminishing of $\Delta M_{F,S}$ for smaller C_F/C_S. Another consequence of this oscillatory behaviour is that the disturbance is not a soliton itself (cf also table 4).

The values in table 3 are in general much larger than those in table 1, in particular for the larger values of C_F/C_S. This effect seems to be due to the use of the Lennard–Jones 6–12 potential and not to a collective phenomenon such as described in the foregoing paragraph.

Finally, one may ask whether the effects considered here are due only to the very high energy of the solitons. Therefore we calculated one series of collisions of solitons of much lower momentum and energy: $M_F = 2{\cdot}91$, $M_S = 1{\cdot}54$, $E_F = 4{\cdot}14$, $E_S = 1{\cdot}11$, $C_F/C_S = 1{\cdot}5$. Note that the energy is in the strongly nonlinear region (cf figure 1) and

Table 5. Relative values of the velocities $\dot{r}_n(t)$ as a function of time for a collision characterised by $C_F/C_S = 1{\cdot}5$ and $d/d_0 = 0{\cdot}77$. Time increases with a step equal to 6×10^{-4}. The actual values are the given ones multiplied by 10^{-2}.

t \ n	1	2	3	4	5	6	7	8	9	10	11
1	0	0	0	0	0	0	0	0	0	0	0
2	70 832	0	0	0	0	0	0	0	0	0	0
3	82 160	10	0	0	0	0	0	0	0	0	0
4	121	82 049	0	0	0	0	0	0	0	0	0
5	35	81 761	409	0	0	0	0	0	0	0	0
6	99 998	4	82 166	0	0	0	0	0	0	0	0
7	1549	98 453	43 186	38 984	0	0	0	0	0	0	0
8	0	99 354	648	82 167	3	0	0	0	0	0	0
9	0	0	99 999	476	81 696	0	0	0	0	0	0
10	0	0	70	99 929	82 066	106	0	0	0	0	0
11	0	0	0	77 514	22 487	82 170	0	0	0	0	0
12	0	0	0	4	99 704	72 705	9759	0	0	0	0
13	0	0	0	4	59	96 257	85 851	1	0	0	0
14	0	0	0	4	52	35 863	49 325	96 928	0	0	0
15	0	0	0	4	52	−83	82 513	97 117	2569	0	0
16	0	0	0	4	52	−83	281	82 123	99 792	4	0
17	0	0	0	4	52	−83	−12	82 229	196	99 786	0
18	0	0	0	4	52	−83	−12	6	82 392	40 306	59 507
19	0	0	0	4	52	−83	−12	−1	63 844	18 555	99 772
20	0	0	0	4	52	−83	−12	−1	0	82 397	5
21	0	0	0	4	52	−83	−12	−1	0	1036	81 363
22	0	0	0	4	52	−83	−12	−1	0	0	82 343
23	0	0	0	4	52	−83	−12	−1	0	0	19

Table 6. Relative values of the velocities $\dot{r}_n$ and energies

$$E_n(t) = \tfrac{1}{2}\dot{r}_n^2 + \tfrac{1}{2}(\tilde{V}(r_{n+1} - r_n) + \tilde{V}(r_n - r_{n-1}) - 2\tilde{V}(0))$$

of particles that take part of the disturbance at a fixed time after the collision of the solitons. The velocity ratio C_F/C_S equals $1{\cdot}15$. The time is chosen in such a way that the disturbance is separated completely from the solitons (see also table 5). The actual values are the given ones multiplied by 10^{-2} and 5×10^{-3} respectively.

	Velocity							Energy						
d/d_0	n	$n+1$	$n+2$	$n+3$	$n+4$	$n+5$	$n+6$	n	$n+1$	$n+2$	$n+3$	$n+4$	$n+5$	$n+6$
0·97	0	6	78	−79	−6	0	0	7	7	67	70	7	7	7
0·77	0	4	52	−83	−12	−1	0	7	7	34	76	8	7	7
0·51	0	2	27	−7	−25	−2	0	7	7	14	7	13	7	7

that these values are of the same order as the difference quantities ΔM_F, etc, in the former case. After collision there again appear two solitons, and

$$|\Delta M_{FR}| < 5\times10^{-5} \qquad |\Delta M_{SR}| < 3\times10^{-4} \qquad |\Delta M_{TR}| < 10^{-4}$$
$$|\Delta E_{FR}| < 10^{-4} \qquad |\Delta E_{SR}| < 4\times10^{-4} \qquad |\Delta E_{TR}| < 10^{-4}.$$

Further, we again found the oscillatory behaviour of the curves ΔM_F, etc, so there are no essential differences with the high-energy case.

Acknowledgments

The authors would like to thank Professor W J Caspers for a critical reading of the manuscript and Mr P Kops for drawing the figures.

References

Batteh J H and Powell J D 1978 *J. Appl. Phys.* **49** 3933–40
Hardy J R and Karo A M 1977 *Proc. Int. Conf. on Lattice Dynamics* ed M Balkanski (Paris: Flammarion)
Rolfe T J, Rice R A and Dancz J 1979 *J. Chem. Phys.* **70** 26–33
Toda M 1975 *Phys. Rep.* **18** 1–124
Valkering T P 1978 *J. Phys. A: Math. Gen.* **11** 1885–97